

# Mdm2 and Mdm4 Loss Regulates Distinct p53 Activities

Juan A. Barboza,<sup>1</sup> Tomoo Iwakuma,<sup>1</sup> Tamara Terzian,<sup>1</sup> Adel K. El-Naggar,<sup>2</sup> and Guillermina Lozano<sup>1</sup>

<sup>1</sup>Department of Cancer Genetics, and <sup>2</sup>Department of Pathology, The University of Texas M. D. Anderson Cancer Center, Houston, Texas

## Abstract

**Mutational inactivation of p53 is a hallmark of most human tumors. Loss of p53 function also occurs by overexpression of negative regulators such as MDM2 and MDM4. Deletion of Mdm2 or Mdm4 in mice results in p53-dependent embryo lethality due to constitutive p53 activity. However, Mdm2<sup>-/-</sup> and Mdm4<sup>-/-</sup> embryos display divergent phenotypes, suggesting that Mdm2 and Mdm4 exert distinct control over p53. To explore the interaction between Mdm2 and Mdm4 in p53 regulation, we first generated mice and cells that are triple null for p53, Mdm2, and Mdm4. These mice had identical survival curves and tumor spectrum as p53<sup>-/-</sup> mice, substantiating the principal role of Mdm2 and Mdm4 as negative p53 regulators. We next generated mouse embryo fibroblasts null for p53 with deletions of Mdm2, Mdm4, or both; introduced a retrovirus expressing a temperature-sensitive p53 mutant, p53A135V; and examined p53 stability and activity. In this system, p53 activated distinct target genes, leading to apoptosis in cells lacking Mdm2 and a cell cycle arrest in cells lacking Mdm4. Cells lacking both Mdm2 and Mdm4 had a stable p53 that initiated apoptosis similar to Mdm2-null cells. Additionally, stabilization of p53 in cells lacking Mdm4 with the Mdm2 antagonist nutlin-3 was sufficient to induce a cell death response. These data further differentiate the roles of Mdm2 and Mdm4 in the regulation of p53 activities. (Mol Cancer Res 2008;6(6):947–54)**

## Introduction

Proper p53 control is critical for its tumor suppressive function. Under homeostatic conditions, p53 is maintained at low levels by the E3 ubiquitin ligase Mdm2, which catalyzes

p53 ubiquitination, marking it for degradation by the proteasome (1-3). Mdm2 also binds and inhibits the p53 transcriptional activation domain (4, 5). In response to DNA damage, p53 phosphorylation disrupts Mdm2 binding, leading to p53 stabilization and activation (6). The importance of Mdm2 in p53 regulation was shown *in vivo* by the lethality of Mdm2<sup>-/-</sup> embryos at 3.5 days postcoitum whereas p53<sup>-/-</sup>Mdm2<sup>-/-</sup> mice develop without abnormalities (7, 8). Mdm2<sup>-/-</sup> blastocysts undergo spontaneous apoptosis, and reintroduction of p53 into p53<sup>-/-</sup>Mdm2<sup>-/-</sup> mouse embryo fibroblasts (MEF) also induces an apoptotic response (9, 10). Similarly, tissue-specific deletion of Mdm2 in cardiomyocytes, smooth muscle cells, and the central nervous system results in p53-dependent apoptosis (11-14). Thus, Mdm2 regulation of p53 is essential for proper development, and loss of Mdm2 is sufficient to induce p53-dependent apoptosis in many cell types.

A homologue of Mdm2, Mdm4, also binds the p53 transactivation domain, inhibiting its activity (15). However, the role of Mdm4 in p53 protein stability is murky at best. Overexpression of MDM4 inhibits MDM2-mediated degradation of p53 in immortalized human tumor cell lines, suggesting that MDM4 stabilizes p53 (16-19). Likewise, loss of Mdm4 in MEFs containing a p53 mutant that lacks the proline-rich domain yielded lower p53 levels, albeit a more active p53 (20). In contrast, MEFs lacking Mdm4 contain elevated p53 levels (21, 22). Tissue-specific deletion of Mdm4 in the central nervous system is also associated with increased p53 immunostaining (12, 14). Two other studies showed that MDM4 contributes to MDM2 E3 ubiquitin ligase activity (23, 24). Gu et al. (25) have shown that the MDM2-to-MDM4 ratio may affect p53 stability, providing a possible explanation for these seemingly conflicting results. MDM4 protects p53 from degradation when overexpressed at a ratio greater than 2:1 with respect to MDM2. However, when expressed at similar levels, MDM4 inhibits MDM2 autoubiquitination and enhances MDM2 degradation of p53.

Deletion of Mdm2 or Mdm4 *in vivo* yields cell lethal phenotypes by different mechanisms (7, 8, 21, 22, 26). As indicated, loss of Mdm2 results in apoptosis in all cells examined to date. Examination of embryos from two Mdm4 mutant lines revealed proliferation defects (22, 26). However, the Mdm4 mutants generated by Migliorini et al. (22) also display apoptosis but only in the developing central nervous system. Conditional deletion of Mdm4 specifically in the central nervous system results in a proliferative defect and apoptosis, whereas cells lacking Mdm2 undergo apoptosis (12, 14). Adult cardiomyocytes lacking Mdm4 also die with time (27). These data suggest that Mdm2 and Mdm4 affect p53 activity differently, resulting in distinct p53 functions in different cell types.

Received 9/25/07; revised 2/1/08; accepted 2/6/08.

**Grant support:** NIH grant CA47296 (G. Lozano) and Cancer Center Support grant CA16672 to M. D. Anderson Cancer Center. J.A. Barboza was supported by Cancer Genetics training grant CA009299.

The costs of publication of this article were defrayed in part by the payment of page charges. This article must therefore be hereby marked *advertisement* in accordance with 18 U.S.C. Section 1734 solely to indicate this fact.

**Note:** Current address for J.A. Barboza: Division of Immunology, Seattle Children's Hospital Research Institute, Seattle, WA 98109. Current address for T. Iwakuma: Department of Genetics/Cancer Center, Louisiana State University Health Science Center, 533 Bolivar Street, New Orleans, LA 70112.

**Requests for reprints:** Guillermina Lozano, Department of Cancer Genetics, The University of Texas M. D. Anderson Cancer Center, 1515 Holcombe Boulevard, Houston, TX 77030-4095. Phone: 713-834-6386; Fax: 713-834-6380. E-mail: ggzozano@mdanderson.org

Copyright © 2008 American Association for Cancer Research.

doi:10.1158/1541-7786.MCR-07-2079

We decided to probe the molecular aspects of this regulation in a different system where we could actually measure p53 half-life. To accomplish this goal, we first asked whether we could generate mice and cells lacking all three genes. Mice lacking *p53*, *Mdm2*, and *Mdm4* were viable but succumbed to tumorigenesis at a rate similar to that of *p53*<sup>-/-</sup> mice. Primary MEFs null for *p53* with varying *Mdm* genotypes were established and infected with a retrovirus encoding a temperature-sensitive p53 mutant. In this system, loss of *Mdm2* or *Mdm4* led to p53-dependent apoptosis or cell cycle arrest, respectively. In addition, p53 exhibited transcriptional activation of distinct p53 target genes in cells lacking *Mdm2* or *Mdm4*. Analysis of p53 protein half-life revealed that Mdm4 protected p53 from Mdm2-mediated degradation. Understanding the mechanisms by which Mdm2 and Mdm4 regulate p53 is essential to maximize their potential as therapeutic targets for reactivating p53 in tumors.

## Results

### Mice Lacking p53, Mdm2, and Mdm4 Are Viable

To explore the genetic interaction between Mdm2 and Mdm4 in regulating p53 activity, we attempted to generate mice and cells lacking all three genes. We crossed *p53*<sup>-/-</sup>*Mdm2*<sup>-/-</sup>*Mdm4*<sup>+/-</sup> and *p53*<sup>-/-</sup>*Mdm2*<sup>-/-</sup>*Mdm4*<sup>+/-</sup> mice to generate *p53*<sup>-/-</sup>*Mdm2*<sup>-/-</sup>*Mdm4*<sup>-/-</sup> mice. Triple-null mice were viable and born according to the expected Mendelian ratio (Table 1). Moreover, *p53*<sup>-/-</sup>*Mdm2*<sup>-/-</sup>*Mdm4*<sup>-/-</sup> bred well and were subsequently crossed to generate a cohort of triple-null mice. These mice succumbed to tumorigenesis at a rate similar to that of *p53*<sup>-/-</sup> mice. Triple-null and *p53*<sup>-/-</sup> mice had a mean survival of 135 and 140 days, respectively ( $P = 0.75$ ; Fig. 1A). Triple-null mice also developed mainly thymic lymphomas (67%) and sarcomas (33%), with a few mice presenting with more than one tumor, similar to *p53*<sup>-/-</sup> mice (Fig. 1B; Table 2; refs. 28, 29). Thus, the comparable survival and tumor incidence of *p53*<sup>-/-</sup>*Mdm2*<sup>-/-</sup>*Mdm4*<sup>-/-</sup> and *p53*<sup>-/-</sup> mice showed that the principal role of Mdm2 and Mdm4 was proper control of p53 activity.

### Loss of Mdm2 or Mdm4 Determines p53 Protein Levels

To analyze the effects of *Mdm2* and *Mdm4* loss on p53 stability and function, we generated isogenic primary MEFs. Because *Mdm2*<sup>-/-</sup> and *Mdm4*<sup>-/-</sup> embryos are not viable, we isolated fibroblasts from *p53*<sup>-/-</sup>*Mdm2*<sup>-/-</sup>, *p53*<sup>-/-</sup>*Mdm4*<sup>-/-</sup>, and *p53*<sup>-/-</sup> embryos and infected them with a retrovirus

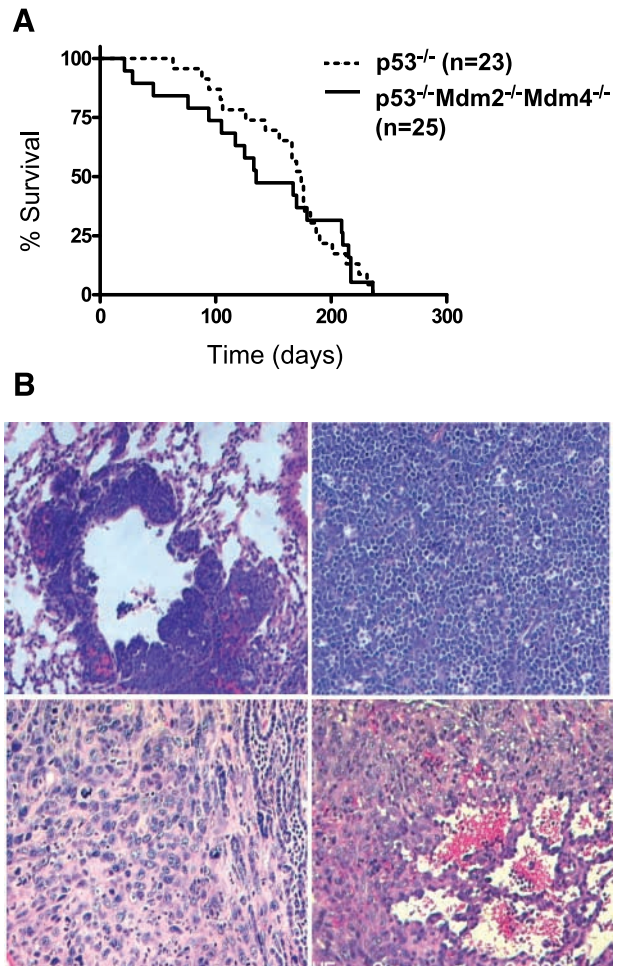


**FIGURE 1.** A. Survival curves of *p53*<sup>-/-</sup> ( $n = 23$ ) and *p53*<sup>-/-</sup>*Mdm2*<sup>-/-</sup>*Mdm4*<sup>-/-</sup> ( $n = 25$ ) mice as determined by Kaplan-Meier analysis. B. Representative tumors arising in *p53*<sup>-/-</sup>*Mdm2*<sup>-/-</sup>*Mdm4*<sup>-/-</sup> mice. Clockwise from top left corner: lymphoma in the lung, thymic lymphoma, angiosarcoma, and a sarcoma adjacent to a lymphoma in the same mouse.

encoding a temperature-sensitive p53 mutant, *p53A135V*. The cells were maintained and characterized as populations and are hereafter referred to as TSA2, TSA4, and TS cells, respectively. The *p53A135V* allele resembles a *p53*-null allele *in vivo* (30). In cells, ~80% of p53A135V resides in the cytoplasm in a

**Table 1. Generation of *p53*<sup>-/-</sup>*Mdm2*<sup>-/-</sup>*Mdm4*<sup>-/-</sup> Mice**

	<i>p53</i> <sup>-/-</sup> <i>Mdm2</i> <sup>-/-</sup> <i>Mdm4</i> <sup>+/-</sup>	×	<i>p53</i> <sup>-/-</sup> <i>Mdm2</i> <sup>-/-</sup> <i>Mdm4</i> <sup>+/-</sup>
Genotype	Expected		Observed ( $P = 0.78$ )
<i>p53</i> <sup>-/-</sup> <i>Mdm2</i> <sup>-/-</sup> <i>Mdm4</i> <sup>+/-</sup>	6		7
<i>p53</i> <sup>-/-</sup> <i>Mdm2</i> <sup>-/-</sup> <i>Mdm4</i> <sup>+/+</sup>	3		3
<i>p53</i> <sup>-/-</sup> <i>Mdm2</i> <sup>-/-</sup> <i>Mdm4</i> <sup>-/-</sup>	3		2
	<i>p53</i> <sup>-/-</sup> <i>Mdm2</i> <sup>-/-</sup> <i>Mdm4</i> <sup>+/-</sup>	×	<i>p53</i> <sup>-/-</sup> <i>Mdm2</i> <sup>-/-</sup> <i>Mdm4</i> <sup>-/-</sup>
Genotype	Expected		Observed ( $P = 0.71$ )
<i>p53</i> <sup>-/-</sup> <i>Mdm2</i> <sup>-/-</sup> <i>Mdm4</i> <sup>+/-</sup>	3.5		4
<i>p53</i> <sup>-/-</sup> <i>Mdm2</i> <sup>-/-</sup> <i>Mdm4</i> <sup>-/-</sup>	3.5		3

NOTE: Two different crosses were set up to examine the combined effects of *Mdm2*, *Mdm4*, and *p53* loss on survival. All possible genotypes of progeny are shown.  $P$  values were determined by  $\chi^2$  test.

**Table 2. Tumor Spectrum of  $p53^{-/-}Mdm2^{-/-}Mdm4^{-/-}$  Mice**

Tumor Types	Tumor Totals
Lymphoma, <i>n</i> (%)	14 of 21 (67)
Sarcoma, <i>n</i> (%)	7 of 21 (33)
Osteosarcoma	1
Spindle cell	1
Epithelioid	1
Angiosarcoma	2
Unclassified	2
Total	21

NOTE: *n* = 19; two animals developed both a lymphoma and sarcoma.

nonfunctional conformation at 39°C, whereas at 32°C it migrates to the nucleus and exhibits wild-type conformation and function (31,32). This enabled us to approximate  $Mdm2^{-/-}$  and  $Mdm4^{-/-}$  contexts at the permissive temperature of 32°C.

To confirm comparable infection of cells, we measured *p53A135V* mRNA expression by real-time reverse transcription-PCR in TS, TSΔ2, and TSΔ4 cells. At the nonpermissive temperature, all three cell populations expressed comparable *p53A135V* mRNA levels and, thus, similar infection efficiency (Fig. 2A). To determine if *p53A135V* was localized as expected (31), we carried out indirect immunofluorescent staining for p53. At 39°C, *p53A135V* was predominantly localized in the cytoplasm of TS, TSΔ2, and TSΔ4 cells and relocalized to the nucleus by 6 hours at 32°C (Fig. 2B). p53 was readily detected in TSΔ2 cells with an exposure of 0.5 seconds. However, the levels of p53 were very low in TS and TSΔ4 cells, requiring 2-second exposures. Western blotting confirmed a difference in the steady-state levels of *p53A135V* protein among cells with different genotypes (Fig. 2C). The level of p53 was 2.6-fold higher in cells lacking *Mdm2* than in control cells. Moreover, the level of p53 was distinctly lower in TSΔ4 cells (0.3-fold) than in TS cells. By comparison to endogenous p53 levels in wild-type MEFs, the levels of *p53A135V* were higher in TS cells (Fig. 2D). Because cell manipulations often lead to activation and stabilization of p53, this system may represent an activated p53. We could not detect endogenous *Mdm2* or *Mdm4* by Western blot analysis in any of these cell populations.

*Mdm4* stabilizes p53 presumably by inhibiting p53-*Mdm2* interactions because *Mdm2* and *Mdm4* bind the same domain of p53 (15-19). However, other reports implicate *Mdm4* in the down-regulation of p53 protein levels (22, 33). To address the effects of *Mdm4* loss on p53 stability, we measured *p53A135V* protein half-life in TSΔ4 cells. TS, TSΔ2, and TSΔ4 cells were cultured at 32°C for 6 hours to allow for conversion of *p53A135V* to its wild-type conformation, treated with cycloheximide, and monitored for p53 levels by Western blotting. In control TS cells, *p53A135V* protein half-life was ~60 minutes (Fig. 3). In the absence of *Mdm2*, *p53A135V* protein levels remained constant throughout the 120-minute time course examined. In contrast, in the absence of *Mdm4*, *p53A135V* was quickly degraded and had a half-life of <15 minutes. Thus, the loss of *Mdm4* resulted in a decrease in *p53A135V* steady-state levels and a drastic reduction in *p53A135V* protein half-life, whereas loss of *Mdm2* stabilized *p53A135V*. We, next introduced *p53A135V* into  $p53^{-/-}Mdm2^{-/-}Mdm4^{-/-}$

(TSΔ2Δ4) MEFs. In these cells, *p53A135V* was stable throughout the 120-minute time course of cycloheximide treatment, similar to the stability of *p53A135V* in TSΔ2 cells (Fig. 3). Thus, in the absence of *Mdm4*, decreased *p53A135V* stability was due to *Mdm2* as deletion of both *Mdm2* and *Mdm4* resulted in a very stable p53 protein.

#### Loss of *Mdm2* or *Mdm4* Determines Distinct p53 Phenotypes

We have previously shown that expression of *p53A135V* in  $p53^{-/-}Mdm2^{-/-}$  MEFs recapitulates the *in vivo* apoptotic phenotype of *Mdm2*-null blastocysts (9, 10). Accordingly, we wished to determine if *p53A135V* expression in TSΔ4 cells could reproduce the proliferation or apoptotic defects seen in  $Mdm4^{-/-}$  embryos (9, 22, 26). We therefore analyzed p53

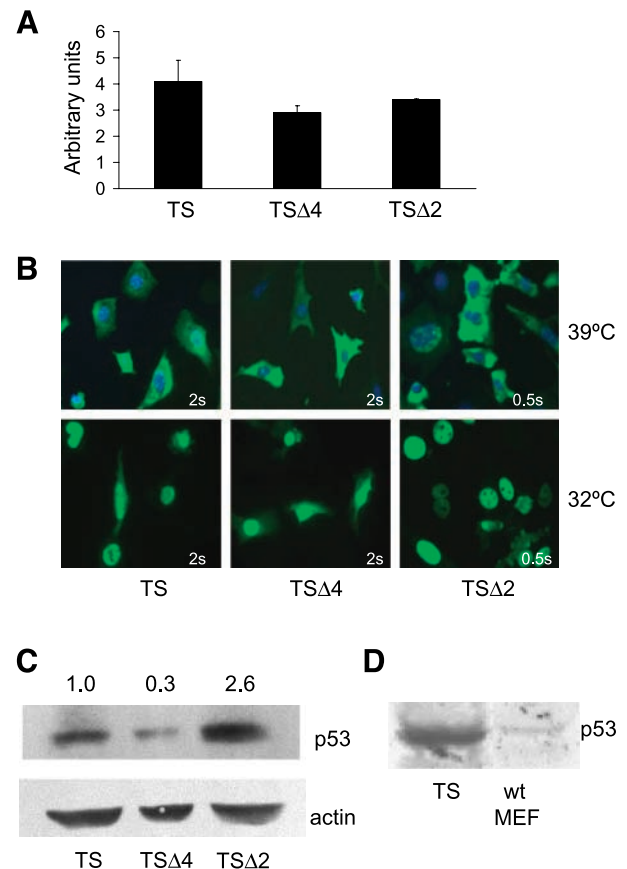


**FIGURE 2.** Endogenous *Mdm2* and *Mdm4* have distinct effects on steady-state p53 levels. **A.** Relative p53 mRNA levels of the temperature-sensitive mutant *p53A135V* were determined by real-time reverse transcription-PCR using RNA from TS, TSΔ4, and TSΔ2 cells cultured at the nonpermissive temperature of 39°C and normalized to a *Gapdh* internal control. SDs were determined from triplicate samples. **B.** TS, TSΔ4, and TSΔ2 cells were cultured at 39°C or 32°C for 6 h, fixed, and incubated with a p53 primary antibody and a FITC-conjugated secondary antibody (green). Nuclei were counterstained with 4',6-diamidino-2-phenylindole (blue). Exposure times are indicated. **C.** Immunoblot of p53 from whole-cell lysates prepared from MEFs after culturing at 32°C for 6 h. β-Actin was used as a loading control. Protein levels were determined by densitometric quantification of immunoblots and relative p53 level is shown. **D.** A comparison of wild-type (*wt*) p53 protein levels in MEFs to *p53A135V* protein levels after retroviral infection of *p53*-null MEFs by Western blot analysis. Equal amounts of total protein were loaded.

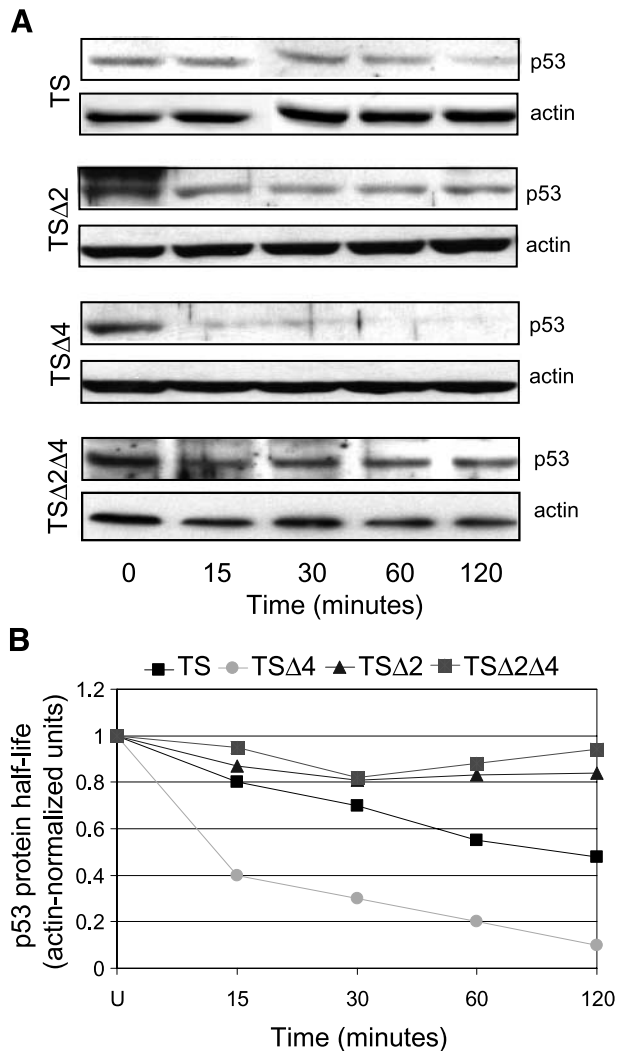


**FIGURE 3.** Endogenous Mdm2 and Mdm4 have distinct effects on p53 protein stability. **A.** TS, TS $\Delta$ 2, TS $\Delta$ 4, and TS $\Delta$ 2 $\Delta$ 4 MEFs were cultured at 32°C for 6 h. Cells were then cultured in the presence of cycloheximide for the indicated times. Cell lysates were prepared and analyzed by immunoblotting with a p53 antibody.  $\beta$ -Actin was used as a loading control. **B.** p53 half-life was determined by densitometric quantification of the representative immunoblots depicted in **A**. Cycloheximide experiments were done at least thrice for each cell population.

initiation of cell cycle arrest and apoptosis after temperature shift in TS, TS $\Delta$ 2, TS $\Delta$ 4, and TS $\Delta$ 2 $\Delta$ 4 cells. We confirmed apoptosis in TS $\Delta$ 2 cells by Annexin V labeling, which detects cell membrane disruption, an early hallmark of apoptosis. Sixty-six percent of TS $\Delta$ 2 cells stained positive for Annexin V 12 hours after temperature shift, whereas TS and TS $\Delta$ 4 cells exhibited negligible Annexin V-FITC reactivity even after 72 hours at 32°C (Fig. 4A and data not shown). Thus, p53A135V induced apoptosis in the absence of Mdm2, but had little effect in cells lacking Mdm4. We next examined the phenotype of TS $\Delta$ 2 $\Delta$ 4 cells after temperature shift. Cells lacking Mdm2 and Mdm4 underwent p53-dependent cell death similar to TS $\Delta$ 2 cells (Fig. 4A and B). Thus, additional loss of Mdm2 in the absence of Mdm4 stabilized p53 and induced

an apoptotic response. These data indicated that the dominant phenotype, apoptosis, was due to loss of Mdm2 and was independent of Mdm4.

We next determined the ratio of G<sub>1</sub>- to S-phase cells at permissive and nonpermissive temperatures. At 39°C, the G<sub>1</sub>-to-S ratio of TS and TS $\Delta$ 4 cells was 0.8 whereas that of TS $\Delta$ 2 cells was 1.5 (Fig. 4C). TS $\Delta$ 2 $\Delta$ 4 cells had a G<sub>1</sub>-to-S ratio of 2.1. Temperature shift to 32°C for 24 hours had a small effect on the number of TS, TS $\Delta$ 2, TS $\Delta$ 4, and TS $\Delta$ 2 $\Delta$ 4 cells in G<sub>1</sub>. However, a pronounced G<sub>1</sub> cell cycle arrest was evident at 48 hours in TS $\Delta$ 4 and TS $\Delta$ 2 as indicated by their G<sub>1</sub>-to-S ratios of 3.7 and 3.5, respectively. Similarly, TS $\Delta$ 2 $\Delta$ 4 cells had a G<sub>1</sub>-to-S ratio of 4.3. Although TS $\Delta$ 2 and TS $\Delta$ 2 $\Delta$ 4 cells exhibited a high G<sub>1</sub>-to-S ratio at 48 hours at 32°C, this represented a small number of cells because the majority of these cells had already died by apoptosis (Fig. 4A and B). In sum, the predominant phenotype in cells lacking Mdm4 was a G<sub>1</sub> cell cycle arrest in response to p53 activation, whereas cells lacking Mdm2, regardless of the Mdm4 genotype, readily underwent apoptosis.

#### Loss of Mdm2 or Mdm4 Enhances Transcriptional Activity of Distinct p53 Targets

Both Mdm2 and Mdm4 bind the p53 amino terminus, inhibiting its transcriptional activity (15, 34). Although loss of Mdm4 rendered p53 unstable, it still caused a p53-dependent cell cycle arrest likely due to enhanced p53 transcriptional activation. To assess p53 transcriptional activity, we measured induction of endogenous *p21*, *Mdm2*, *cyclin G*, *Bax*, *Perp*, and *Noxa* mRNAs by quantitative real-time reverse transcription-PCR. TS, TS $\Delta$ 2, and TS $\Delta$ 4 cells were cultured at 39°C or 32°C for 6 and 12 hours and then harvested for analysis. Interestingly, TS $\Delta$ 4 cells exhibited a 5-fold increase in *Mdm2* levels over TS cells by 6 hours at 32°C (Fig. 5A). In addition, *p21* was induced 2.5-fold by 12 hours after temperature shift (Fig. 5B). However, there was no induction of *cyclin G*, *Bax*, *Perp*, and *Noxa* in the absence of Mdm4. The gene expression profiles were different in TS $\Delta$ 2 cells; these cells expressed *Perp* 3-fold over control cells at 39°C and 6-fold higher after temperature shift for 6 hours (Fig. 5C). *Noxa* was also expressed 3-fold higher than in controls at 32°C and *p21* mRNA levels were slightly elevated over control cells 12 hours after temperature shift (Fig. 5D). Expression of *cyclin G* and *Bax* did not change in TS $\Delta$ 2 cells. These findings indicated that in the absence of Mdm4, p53A135V activated *Mdm2* and *p21*. In contrast, the apoptotic genes *Perp* and *Noxa* were preferentially up-regulated in TS $\Delta$ 2 cells. Our results suggested that Mdm2 and Mdm4 determined initiation of cell cycle arrest or apoptosis by controlling p53 transcriptional activation of distinct target genes.

#### Disruption of Mdm2/p53 Interaction Stabilizes p53 and Initiates Apoptosis in the Absence of Mdm4

Various factors such as the cellular context and p53 protein levels have been shown to influence p53 initiation of a cell cycle arrest or apoptosis (35). Our data suggest that in MEFs, protein levels regulated p53 response. To directly test whether enhanced p53 protein levels were sufficient to induce cell death, we treated TS and TS $\Delta$ 4 cells with the Mdm2 antagonist nutlin-3 (36). Cells were cultured at 32°C for 4 hours and for an

additional 4 hours in the presence of nutlin-3. Treatment with nutlin-3a caused p53A135V stabilization in both TS and TSΔ4 cells (Fig. 6A). In TSΔ4 cells, however, stabilization is specifically due to loss of p53 interactions with Mdm2 because these cells do not have Mdm4. Moreover, nutlin-3a, but not the inactive enantiomer nutlin-3b, reduced the viability of both cell types. Treatment with nutlin-3a caused cell death in ~28% of TS cells and 42% of TSΔ4 cells at 4 hours (Fig. 6B). Thus, treatment of primary murine fibroblasts with the Mdm2 antagonist nutlin-3a stabilized p53 and was sufficient to induce a cell death response independent of *Mdm4*.

## Discussion

Knowledge of the mechanisms by which p53 chooses to initiate apoptosis or cell cycle arrest is critical to understanding tumor response on reactivation of p53 (37-39). Clearly, context is important in this decision, but we wanted to further these studies to examine the molecular aspects of this decision.

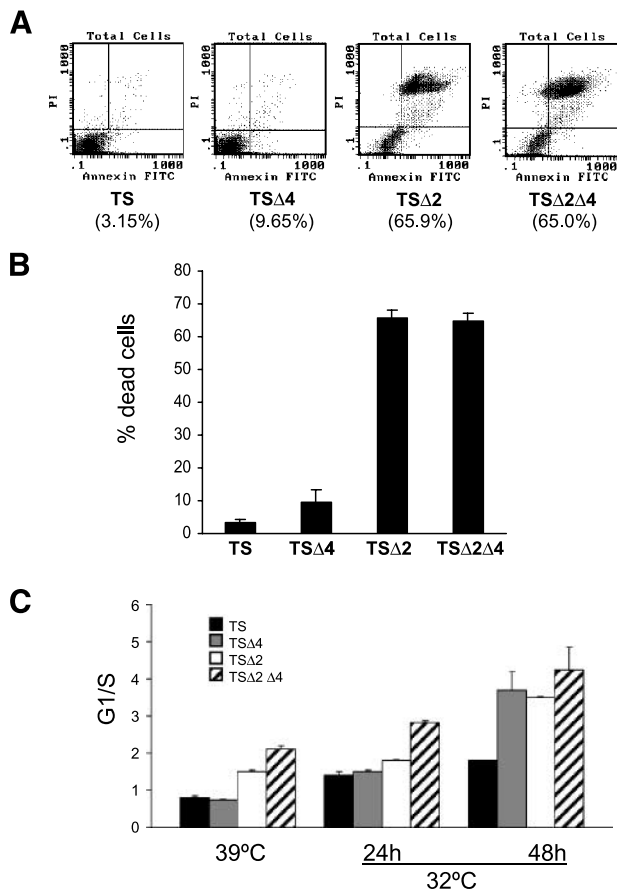


**FIGURE 4.** Mdm2 and Mdm4 determine p53 initiation of cell cycle arrest or apoptosis. **A.** MEFs were cultured at 32°C for 12 h, labeled with Annexin V-fluorescein and propidium iodide, and analyzed by flow cytometry to determine cell viability. Percentages represent apoptotic cells (Annexin V positive). **B.** Cell viability as determined by positive Annexin V staining described in **A.** **C.** The G<sub>1</sub>-to-S ratio was calculated from cells cultured at 39°C and 32°C and analyzed by flow cytometry. Columns, mean from at least three independent experiments done in duplicate; bars, SE.

To examine the roles of Mdm2 and Mdm4 in this process, we first recapitulated *Mdm2*<sup>-/-</sup>, *Mdm4*<sup>-/-</sup>, and double-null contexts by expression of a temperature-sensitive p53 protein in primary MEFs. Although various studies have shown that MDM4 overexpression stabilizes p53 in tumor-derived cell lines (16-19, 40), we show that endogenous levels of Mdm4 are sufficient to stabilize p53A135V from Mdm2-mediated degradation because loss of *Mdm4* resulted in reduced p53A135V protein half-life. Thus, in these studies, the levels of Mdm4 overwhelm the amount of Mdm2 present in the cell, resulting in p53A135V stabilization. Because Mdm2 and Mdm4 bind the same domain of p53, p53A135V stabilization likely resulted from Mdm4 impeding Mdm2 access to p53A135V (5, 15). Importantly, various studies have shown that Mdm2-Mdm4 interactions also regulate p53 stability and function. In human cells, Mdm4 (also called Hdmx) enhances Mdm2 (also called Hdm2) ligase activity and p53 degradation (40). On the basis of structural analysis, Kostic et al. (41) proposed that Mdm2 and Mdm4 heterodimerization via their respective RING domains contributes to enhanced Mdm2 activity. DNA damage also redirects the ligase activity of Mdm2 from p53 to itself and Mdm4, facilitating p53 activation (42). Therefore, cellular context becomes important as the ratios of Mdm2, Mdm4, and p53 might favor Mdm4-p53, Mdm2-p53, or Mdm4-Mdm2 complexes, resulting in p53 stabilization or degradation. Whereas we know that *Mdm2* is transcriptionally regulated by p53, little is known about the transcriptional regulation of *Mdm4* (43). Further studies of the interactions of these proteins under specific conditions as well as identification of modifications conducive to particular interactions are needed to further understand the mechanisms of p53 response.

In our studies, a very unstable p53A135V in the absence of *Mdm4* retained some transcriptional activity. In TSΔ4 cells, *Mdm2* was robustly and rapidly induced by p53A135V after temperature shift, indicating that the initial response to enhanced p53 activity may be to restore physiologic p53 levels. The cell cycle inhibitor p21 was also activated, and these cells exhibited a G<sub>1</sub>-S arrest. Although MEFs lacking *Mdm4* exhibited enhanced p53 activity, these cells did not undergo apoptosis. Under the same conditions, MEFs lacking *Mdm2* expressed a stable p53A135V and readily underwent apoptosis at 32°C. Furthermore, cells lacking both *Mdm2* and *Mdm4* died by apoptosis, suggesting that *Mdm2* loss and p53 stabilization are the critical determinants of apoptosis in this system. This idea was further supported by the observation that stabilization of p53A135V on treatment of TS and TSΔ4 cells with the Mdm2 antagonist nutlin-3a also induced a prompt cell death response. Thus, stabilization of p53A135V was associated with the activation of apoptotic target genes and was sufficient to induce apoptosis. The prediction then is that tumors will undergo apoptosis if p53 levels are high enough.

Remarkably, mice lacking *p53*, *Mdm2*, and *Mdm4* were viable. Furthermore, loss of all three genes did not exacerbate the tumorigenic effect of *p53* loss alone, indicating that the primary *in vivo* role of endogenous Mdm2 and Mdm4 levels was control of p53 activity. Nevertheless, the distinct effects of Mdm4 on p53 stability, activity, and function underscore its potential as another mechanism for inactivating p53 in human tumors (44).

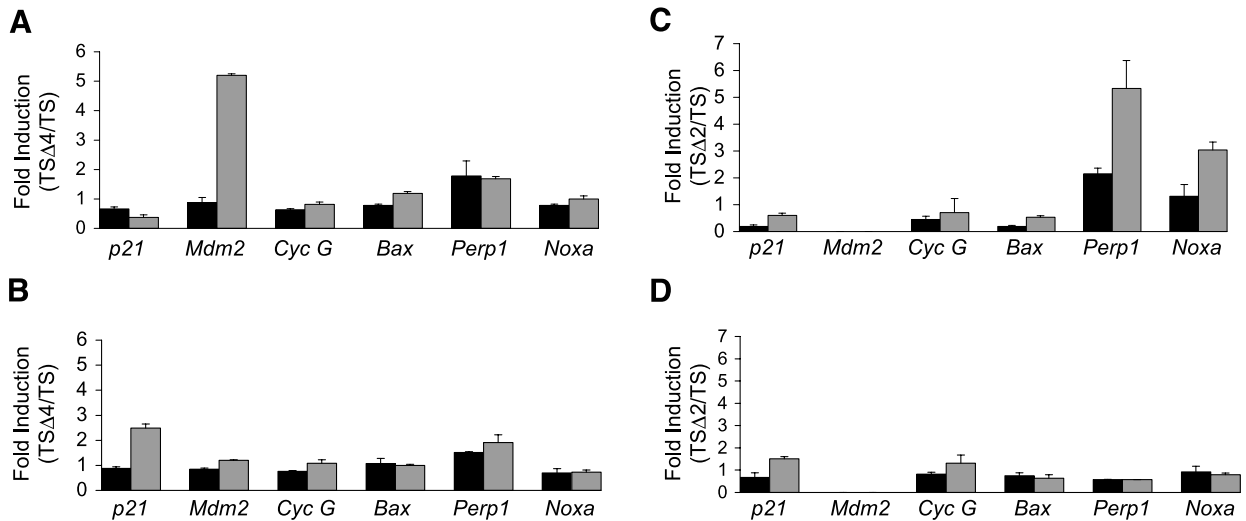


**FIGURE 5.** Transcriptional activation of p53 target genes in TS, TS $\Delta$ 2, and TS $\Delta$ 4 MEFs. Fold induction was calculated as gene expression in TS $\Delta$ 4 cells over TS cells 6 h (A) and 12 h (B) after temperature shift, and in TS $\Delta$ 2 cells over TS cells 6 h (C) and 12 h (D) after temperature shift. Values were normalized to expression of *Gapdh* in each reaction. Columns, mean from three independent experiments done in duplicate; bars, SE.

## Materials and Methods

### Mice and Cell Culture

Generation of *Mdm4*<sup>-/-</sup> and *Mdm2*<sup>-/-</sup> mice was previously described (8, 26). Mice were crossed with C57BL/6 mice for more than five generations until the background was >90% C57BL/6. MEFs were derived from 13.5-d-old embryos and maintained

in DMEM supplemented with 10% fetal bovine serum and 1% antibiotics. 293 Eco Pac packaging cells (Clontech) were maintained per manufacturer's recommendations. Twenty-four hours after plating, packaging cells were transfected with 3  $\mu$ g of pBabe empty vector or pBabe-p53A135V using Fugene 6 reagent (Roche). For retroviral transduction of MEFs, viral supernatants from 293 cells were applied to early passage (P0-P5) MEFs in the presence of polybrene (4  $\mu$ g/mL). Infected MEFs were cultured at 39°C for 24 to 48 h to allow for infection, and then media were supplemented with puromycin (2.5  $\mu$ g/mL) for selection. Confluent puromycin-resistant pools of cells were split into duplicate dishes and either cultured at 32°C or 39°C and harvested for analysis at the indicated times. Infected cells were continuously cultured in the presence of puromycin. For nutlin experiments, 50  $\mu$ mol/L of nutlin-3a or nutlin-3b (kindly provided by Michael Andreeff, The University of Texas M. D. Anderson Cancer Center, Houston, TX) was used.

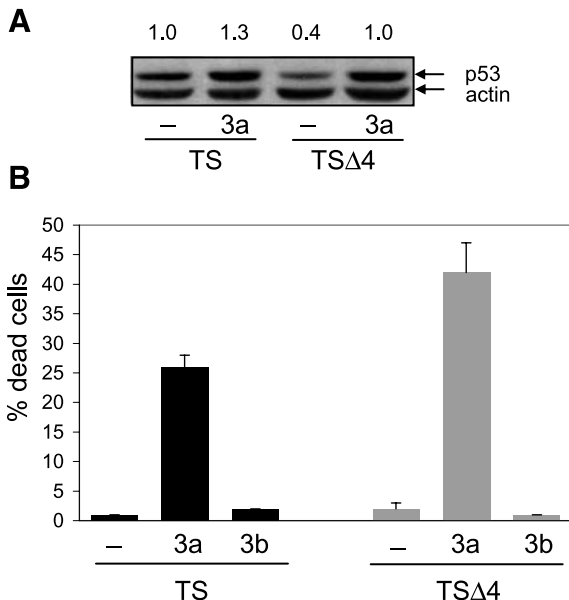


**FIGURE 6.** p53 stabilization induces a cell death response independent of *Mdm4*. **A.** TS and TS $\Delta$ 4 MEFs were cultured at 32°C for 4 h, treated with 50  $\mu$ mol/L nutlin-3a for 1 h, and analyzed for p53 expression by immunoblotting. Protein levels were determined as in Fig. 1C and relative p53 levels are shown. **B.** MEFs were cultured at 32°C for 4 h and then treated with 50  $\mu$ mol/L of nutlin-3a or nutlin-3b for an additional 4 h. Cell viability was determined by trypan blue exclusion. At least 200 cells were counted for each treatment. Columns, mean from two independent experiments done in duplicate; bars, SE.

### Flow Cytometry and Annexin V Assay

MEFs were harvested by trypsinization, washed in PBS, and then fixed with cold 70% ethanol. On the day of analysis, cells were washed with PBS-T (0.1% Triton X-100), incubated with p53 antibody FL-393 (1:100; Santa Cruz Biotechnology) for 30 min at room temperature, and then incubated with FITC-conjugated secondary antibody (1:400) for 1 h. After washing, cells were incubated with 50  $\mu$ g/mL propidium iodide in PBS-T (1% Triton X-100) and analyzed by flow cytometry on a Coulter Counter EPICS Profile Analyzer. Annexin V assays were done with an Annexin V-FLUOS kit per manufacturer's recommendations (Roche).

### Immunoblotting and Protein Stability

Cells were harvested by scraping in cold PBS and cell pellets were resuspended in 2 $\times$ SDS loading buffer. Proteins were resolved by electrophoresis on 10% polyacrylamide gels,

transferred onto a nitrocellulose membrane, and blotted with antibodies to p53 (FL-393, Santa Cruz Biotechnology) and  $\beta$ -actin (Sigma). To measure protein stability, cells were cultured in the presence of 30  $\mu$ g/mL cycloheximide (Sigma) for the indicated times and harvested for analysis. Protein levels were quantified by densitometry with a Storm 880 Phosphoimager (Molecular Dynamics).

#### Immunofluorescent Labeling

Cells were cultured under indicated conditions on coverslips in six-well plates, then washed with PBS and fixed with methanol/acetone (50:50%) for 3 min at room temperature. After washing with PBS, cells were incubated with p53 antibody (FL-393) for 16 h at 4°C and then incubated with FITC-conjugated secondary antibody for 1 h. Coverslips were then mounted on slides with mounting media containing 4',6-diamidino-2-phenylindole (Vector Laboratories). Cells were visualized with a Leica Epifluorescence microscope for the indicated exposure times.

#### Quantitative Real-time Reverse Transcription-PCR

RNA was extracted from MEFs using an RNeasy kit (Qiagen). Reverse transcription reactions were done with the First Strand cDNA Synthesis Kit per manufacturer's recommendation (GE Healthcare). Real-time reverse transcription-PCR was done according to the manufacturer's specification (Applied Biosystems). The Primer Express program was used to design primer sequences that were confirmed for specificity by BLASTN. The following primers were used: *Perp*, CAGAGC-CTCATGGAGTACGC and GAGAATGAAGCAGATGCA-CAGG. Sequences of *p21*, *Mdm2*, *cyclin G*, *Bax*, *Noxa*, and *Gapdh* primers were previously described (45, 46). Gene expression was normalized to *Gapdh* expression in each reaction.

#### Disclosure of Potential Conflicts of Interest

No potential conflicts of interest were disclosed.

#### Acknowledgments

We thank Sohela de Rozieres, Young-Ah Suh, Shunbin Xiong, John Parant, and Sean Post for helpful discussions, and Karen Ramirez for help with flow cytometry.

#### References

- Haupt Y, Maya R, Kazaz A, Oren M. Mdm2 promotes the rapid degradation of p53. *Nature* 1997;387:296–9.
- Honda R, Tanaka H, Yasuda H. Oncoprotein MDM2 is a ubiquitin ligase E3 for tumor suppressor p53. *FEBS Lett* 1997;420:25–7.
- Kubbutat MH, Jones SN, Vousden KH. Regulation of p53 stability by Mdm2. *Nature* 1997;387:299–303.
- Momand J, Zambetti GP, Olson DC, George D, Levine AJ. The mdm-2 oncogene product forms a complex with the p53 protein and inhibits p53-mediated transactivation. *Cell* 1992;69:1237–45.
- Oliner JD, Pietenpol JA, Thiagalangam S, Gyuris J, Kinzler KW, Vogelstein B. Oncoprotein MDM2 conceals the activation domain of tumour suppressor p53. *Nature* 1993;362:857–60.
- Shieh SY, Ikeda M, Taya Y, Prives C. DNA damage-induced phosphorylation of p53 alleviates inhibition by MDM2. *Cell* 1997;91:325–34.
- Jones SN, Roe AE, Donehower LA, Bradley A. Rescue of embryonic lethality in Mdm2-deficient mice by absence of p53. *Nature* 1995;378:206–8.
- Montes de Oca Luna R, WD, Lozano G. Rescue of early embryonic lethality in mdm2-deficient mice by deletion of p53. *Nature* 1995;378:203–6.
- Chavez-Reyes A, Parant JM, Amelse LL, de Oca Luna RM, Korsmeyer SJ, Lozano G. Switching mechanisms of cell death in mdm2- and mdm4-null mice by deletion of p53 downstream targets. *Cancer Res* 2003;63:8664–9.
- de Rozieres S, Maya R, Oren M, Lozano G. The loss of mdm2 induces p53-mediated apoptosis. *Oncogene* 2000;19:1691–7.
- Boesten LS, Zadelaar SM, De Clercq S, et al. Mdm2, but not Mdm4, protects terminally differentiated smooth muscle cells from p53-mediated caspase-3-independent cell death. *Cell Death Differ* 2006;13:2089–98.
- Francoz S, Froment P, Bogaerts S, et al. Mdm4 and Mdm2 cooperate to inhibit p53 activity in proliferating and quiescent cells *in vivo*. *Proc Natl Acad Sci U S A* 2006;103:3232–7.
- Grier JD, Xiong S, Elizondo-Fraire AC, Parant JM, Lozano G. Tissue-specific differences of p53 inhibition by Mdm2 and Mdm4. *Mol Cell Biol* 2006;26:192–8.
- Xiong S, Van Pelt CS, Elizondo-Fraire AC, Liu G, Lozano G. Synergistic roles of Mdm2 and Mdm4 for p53 inhibition in central nervous system development. *Proc Natl Acad Sci U S A* 2006;103:3226–31.
- Shvarts A, Steegenga WT, Riteco N, et al. MDMX: a novel p53-binding protein with some functional properties of MDM2. *EMBO J* 1996;15:5349–57.
- Stad R, Ramos YF, Little N, et al. Hdmx stabilizes Mdm2 and p53. *J Biol Chem* 2000;275:28039–44.
- Jackson MW, Berberich SJ. MdmX protects p53 from Mdm2-mediated degradation. *Mol Cell Biol* 2000;20:1001–7.
- Stad R, Little NA, Xirodimas DP, et al. Mdmx stabilizes p53 and Mdm2 via two distinct mechanisms. *EMBO Rep* 2001;2:1029–34.
- Sharp DA, Kratowicz SA, Sank MJ, George DL. Stabilization of the MDM2 oncoprotein by interaction with the structurally related MDMX protein. *J Biol Chem* 1999;274:38189–96.
- Marine JC, Francoz S, Maetens M, Wahl G, Toledo F, Lozano G. Keeping p53 in check: essential and synergistic functions of Mdm2 and Mdm4. *Cell Death Differ* 2006;13:927–34.
- Finch RA, Donoviel DB, Potter D, et al. Zhang N, mdmx is a negative regulator of p53 activity *in vivo*. *Cancer Res* 2002;62:3221–5.
- Migliorini D, Lazzarini Denchi E, Danovi D, et al. Mdm4 (mdmx) regulates p53-induced growth arrest and neuronal cell death during early embryonic mouse development. *Mol Cell Biol* 2002;22:5527–38.
- Poyurovsky MV, Priest C, Kentsis A, et al. The Mdm2 RING domain C-terminus is required for supramolecular assembly and ubiquitin ligase activity. *EMBO J* 2007;26:90–101.
- Uldrijan S, Pannekoek WJ, Vousden KH. An essential function of the extreme C-terminus of MDM2 can be provided by MDMX. *EMBO J* 2007;26:102–12.
- Gu J, Kawai H, Nie L, et al. Mutual dependence of MDM2 and MDMX in their functional inactivation of p53. *J Biol Chem* 2002;277:19251–4.
- Parant J, Chavez-Reyes A, Little NA, Yan W, Reinke V, Jochemsen AG, Lozano G. Rescue of embryonic lethality in Mdm4-null mice by loss of Trp53 suggests a nonoverlapping pathway with MDM2 to regulate p53. *Nat Genet* 2001;29:92–5.
- Xiong S, Van Pelt CS, Elizondo-Fraire AC, Fernandez-Garcia B, Lozano G. Loss of Mdm4 results in p53-dependent dilated cardiomyopathy. *Circulation* 2007;115:2925–30.
- Donehower LA, Harvey M, Slagle BL, et al. Mice deficient for p53 are developmentally normal but susceptible to spontaneous tumours. *Nature* 1992;356:215–21.
- Jacks T, Remington L, Williams BO, et al. Tumor spectrum analysis in p53-mutant mice. *Curr Biol* 1994;4:1–7.
- Nister M, Tang M, Zhang XQ, et al. p53 must be competent for transcriptional regulation to suppress tumor formation. *Oncogene* 2005;24:3563–73.
- Martinez J, Georgoff I, Levine AJ. Cellular localization and cell cycle regulation by a temperature-sensitive p53 protein. *Genes Dev* 1991;5:151–9.
- Michalovitz D, Halevy O, Oren M. Conditional inhibition of transformation and of cell proliferation by a temperature-sensitive mutant of p53. *Cell* 1990;62:671–80.
- Badciong JC, Haas AL. MdmX is a RING finger ubiquitin ligase capable of synergistically enhancing Mdm2 ubiquitination. *J Biol Chem* 2002;277:49668–75.
- Bottger V, Bottger A, Garcia-Echeverria C, et al. Comparative study of the p53–2 and p53-MDMX interfaces. *Oncogene* 1999;18:189–99.
- Oren M. Decision making by p53: life, death and cancer. *Cell Death Differ* 2003;10:431–42.

36. Vassilev LT, Vu BT, Graves B, et al. *In vivo* activation of the p53 pathway by small-molecule antagonists of MDM2. *Science* 2004;303:844–8.
37. Martins CP, Brown-Swigart L, Evan GI. Modeling the therapeutic efficacy of p53 restoration in tumors. *Cell* 2006;127:1323–34.
38. Ventura A, Kirsch DG, McLaughlin ME, et al. Restoration of p53 function leads to tumour regression *in vivo*. *Nature* 2007;445:661–5.
39. Xue W, Zender L, Miething C, et al. Senescence and tumour clearance is triggered by p53 restoration in murine liver carcinomas. *Nature* 2007;445:656–60.
40. Linares LK, Hengstermann A, Ciechanover A, Muller S, Scheffner M. HdmX stimulates Hdm2-mediated ubiquitination and degradation of p53. *Proc Natl Acad Sci U S A* 2003;100:12009–14.
41. Kostic M, Matt T, Martinez-Yamout MA, Dyson HJ, Wright PE. Solution structure of the Hdm2 C2H2C4 RING, a domain critical for ubiquitination of p53. *J Mol Biol* 2006;363:433–50.
42. Wang YV, Wade M, Wong E, Li YC, Rodewald LW, Wahl GM. Quantitative analyses reveal the importance of regulated Hdmx degradation for p53 activation. *Proc Natl Acad Sci U S A* 2007;104:12365–70.
43. Iwakuma T, Lozano G. MDM2, an introduction. *Mol Cancer Res* 2003;1:993–1000.
44. Laurie NA, Donovan SL, Shih CS, et al. Inactivation of the p53 pathway in retinoblastoma. *Nature* 2006;444:61–6.
45. Bruins W, Zwart E, Attardi LD, et al. Increased sensitivity to UV radiation in mice with a p53 point mutation at Ser389. *Mol Cell Biol* 2004;24:8884–94.
46. Wu WS, Heinrichs S, Xu D, et al. Slug antagonizes p53-mediated apoptosis of hematopoietic progenitors by repressing puma. *Cell* 2005;123:641–53.



# Molecular Cancer Research

## ***Mdm2* and *Mdm4* Loss Regulates Distinct p53 Activities**

Juan A. Barboza, Tomoo Iwakuma, Tamara Terzian, et al.

*Mol Cancer Res* 2008;6:947-954.

**Updated version** Access the most recent version of this article at:  
<http://mcr.aacrjournals.org/content/6/6/947>

**Cited articles** This article cites 46 articles, 19 of which you can access for free at:  
<http://mcr.aacrjournals.org/content/6/6/947.full#ref-list-1>

**Citing articles** This article has been cited by 15 HighWire-hosted articles. Access the articles at:  
<http://mcr.aacrjournals.org/content/6/6/947.full#related-urls>

**E-mail alerts** [Sign up to receive free email-alerts](#) related to this article or journal.

**Reprints and Subscriptions** To order reprints of this article or to subscribe to the journal, contact the AACR Publications Department at [pubs@aacr.org](mailto:pubs@aacr.org).

**Permissions** To request permission to re-use all or part of this article, use this link  
<http://mcr.aacrjournals.org/content/6/6/947>.  
Click on "Request Permissions" which will take you to the Copyright Clearance Center's (CCC) Rightslink site.